Spin Coating and Characterization of Thin High-Density Polyethylene Films

O. Mellbring,[†] S. Kihlman Øiseth,[‡] A. Krozer,[§] J. Lausmaa,[#] and T. Hjertberg*,[†]

Department of Polymer Technology, Chalmers University of Technology, SE-412 96 Göteborg, Sweden; Department of Applied Physics, Chalmers University of Technology, SE-412 96 Göteborg, Sweden; Imego Institute, Aschebergsg. 46, SE-411 33 Göteborg, Sweden; and Department of Chemistry & Materials Technology, SP Swedish National Testing and Research Institute, 50115 Borås, Sweden

Received January 20, 2000; Revised Manuscript Received April 11, 2001

ABSTRACT: The properties of thin films (0.03−2 μm) of high-density polyethylene spin-coated at elevated temperatures (100−180 °C) onto silicon wafers and evaporated gold films were investigated. The coatings were characterized with respect to thickness (ellipsometry, QCM), chemical composition (ESCA, TOF-SIMS), and morphology (optical microscopy, AFM). Initial deposition temperature was found to be an important process parameter that affected the crystal morphology, uniformity, and thickness of the films. The nucleation and the crystal growth were found to depend on both the substrate type and surface properties, especially at low supercooling. Below a film thickness of 0.1 μm, the morphology was composed of aggregates of edge-on oriented lamellae instead of the flattened spherulitic structure observed in thicker films. This thickness dependence of the morphology ceased when the spin-coating was performed at the lowest process temperature, since crystallization probably occurred in the presence of solvent, rather than via a polymer melt, which promoted spherulitic growth. Low process temperatures also gave more uniform films and suppressed the formation of surface striations owing to lower solvent evaporation rate.

Introduction

Thin polymer films and polymer surfaces have received more attention in recent years, mainly due to new understanding of their unique properties and to the progress of analytical techniques. Several studies have shown that thin polymer films of submicron thickness, freely standing or supported, exhibit different properties as compared with bulk material. Two decades ago, Prest and Luca[1] observed an increase in birefringence with decreasing film thickness in casted amorphous polymers. They were thus the first to report an in-plane orientation of polymer chains in thin coatings (1−5 μm). Despotopolou et al.[2] found that the degree of crystallinity and the rate of crystallization were reduced in thin films of poly(di-*n*-hexylsilane). Chain confinement effects were also demonstrated by Forrest et al.,[3] who observed a reduction in the glass transition temperature (T_g) of polystyrene in thin films (0.03−0.2 μm), for which they saw a dramatic effect, especially in freely standing films. The work of Muratoglu et al.[4] and Bartczak et al.[5] explaining the toughening mechanism in particle-filled polyamide and HDPE, respectively, are examples of the relevance of thin layers in a more applied sense. The toughening, which occurred at a critical interparticle ligament dimension, was described to be due to a preferred crystal orientation of the polymer chains at the interface.

Besides providing unique features, thin films are a means to facilitate surface analysis, which is important in such areas as biocompatibility and adhesion. Fourier transform infrared spectroscopy−reflection absorption spectroscopy (FTIR−RAS) can be used to determine functional groups in the film. Furthermore, the use of thin film samples can improve the resolution in for example time-of-flight secondary ion mass spectrometry (TOF-SIMS) analysis or electron spectroscopy for chemical analysis (ESCA), since it leads to less charging.

The aim of this work is to create well-defined polymer films that can be used as model substrates for subsequent, systematic surface modification studies, using different techniques such as glow discharge plasma, wet chemistry, and grafting. Polyethylene was chosen as a model material since it is an extensively studied polymer with a relatively simple chemical structure and well-known bulk properties. It is also inexpensive and widely used in industrial applications. In addition, several important properties of polyethylene can be varied, e.g., molecular weight, crystallinity, and polarity (through copolymerization).

Spin coating is a well-established method for preparing smooth polymeric coatings on flat substrates. The technique is used in the microelectronic industry for the photolithographic processing of silicon wafers. Compared with other methods for preparing thin non-cross-linked polymer coatings, such as solution casting[6] and dip coating,[7] spin coating is perhaps the most straightforward, although not a simple procedure for obtaining uniform films of a specific thickness. An alternative but more expensive technique is plasma deposition,[8] which requires a vacuum system and usually invokes a large degree of cross-linking.[9]

Many studies have related spin-coating process parameters to final film properties, and several models have been proposed (see the reviews of Bornside et al.[10] and Lawrence[11]). The process, which eventually leads to a liquid−solid phase transition, is complex and involves time-dependent changes in the properties of the applied solution. Schematically, it can be described as follows. The polymer is dissolved in a suitable solvent and applied on a substrate. By rotating the substrate at high speed, the excess solution is ejected almost instantly, leaving a thin film, which during the next few seconds continues to flow radially owing to the action of centrifugal force. As the film thins down, the solvent evaporates and the viscosity increases to a point at

[†] Department of Polymer Technology, Chalmers University of Technology.
[‡] Department of Applied Physics, Chalmers University of Technology.
[§] Imego Institute.
[#] SP Swedish National Testing and Research Institute.

10.1021/ma000094x CCC: $20.00
Published on Web 09/08/2001

which the film motion stops. The process is completed by evaporation of the remaining solvent. The most important parameters affecting the film thickness are spin speed, volatility of the solvent, and initial polymer concentration, i.e., the viscosity of the solution.

There are several papers on spin coating of amorphous polymers in the literature, but only a few dealing with crystalline polymers.[2,12,13] A crystallization process might lead to an inhomogeneous film with inferior properties. As high-density polyethylene (HDPE) is insoluble at ambient temperatures, spin coating of this polymer calls for the use of increased temperatures, leading to a relatively complex process. This, combined with the obvious interest to use HDPE in thin film applications, motivated us to start this investigation. A study of spin-coated recrystallized thin films of HDPE was recently published by Bartczak et al.[12] They used atomic force microscopy (AFM) and wide-angle X-ray scattering (WAXS) to characterize the structure of films deposited mainly on calcite but also on silicon wafer and ethylene−octene rubber. We have instead focused on the effect of process conditions on the properties of HDPE spin-coated onto differentially pretreated silicon wafers and gold surfaces. During the course of the experiments we found that the morphology of the films had several interesting features, including an obvious substrate dependence.[14]

Experimental Section

Materials. HDPE powder ($\rho = 0.962$ g/cm^3, MFR$_2 = 12$, $M_n = 25\,000$ g/mol, and $M_w = 72\,000$ g/mol according to size exclusion chromatography (SEC)), received from Borealis Stenungsund, Sweden, was dissolved in boiling (180−190 °C) decalin (99+%, Sigma Aldrich) at various concentrations (0.25−5.0 wt %) for at least 2 h. Boiling the polymer in decalin for 6 h resulted in a decrease in the molecular weight by 15% and 30% for M_n and M_w, respectively, as observed with SEC.

Two types of substrates were used in this study: commercial p-doped Si(100) wafers and gold films evaporated onto 0.2 mm thick quartz disks (diameter: 25.4 mm). The latter were the electrodes of quartz crystal microbalance (QCM) disks. The silicon wafers were cut in ca. 5 cm^2 pieces and ultrasonically cleaned in acetone, in 2-propanol, and in deionized, ultrafiltered water (Milli-Q) and blown dry with nitrogen. The gold substrates (QCM disks) were cleaned in 80 °C solution of 25% NH_3, 30% H_2O_2, and Milli-Q water (1:1:5) for 10 min. They were then treated twice with UV/ozone for 10 min and washed with Milli-Q water. In some measurements the surface of both substrates were further modified prior to polymer coating, either by oxygen plasma treatment or by evaporation coating of silicon dioxide (200 and 30 nm thick layer, respectively, on a 10 nm thick layer of titanium). The composition of the silicon dioxide coating was characterized and confirmed by ESCA.

Polymer Film Preparation. Before applying the polymer solution, all necessary equipment (silicon substrates or QCM disks, chucks, and pipets) was preheated to the actual deposition temperature (100−180 °C) of the solution, in an oven close to the spin coater. The transfer of the hot substrate, from oven to spin start, took about 10 s. Immediately after the substrate was completely wetted with the polymer solution, the spin coater was started and run for 1 min. The rotational speed was varied between 800 and 4000 rpm. To investigate the influence of the chuck design on the resulting film, different geometries of holes or troughs in the chucks were used to attach the substrate with light vacuum. A few films were remelted in an oven for 15 min at 180 °C and slowly cooled by turning off the power in the oven (approximate cooling rate: 0.5 °C/min).

Characterization. The as-prepared films were analyzed using the methods described below. ESCA was used to characterize the chemical composition of the surface of the polymer films. Spectra were recorded using a Perkin-Elmer PHI 5000C ESCA system, equipped with a monochromatic Al Kα (1486.6 eV) source, no charge neutralization, and a 45° takeoff angle. Relative atomic concentrations were calculated by the software using PHI sensitivity factors.

Two samples (film thickness 0.05 and 0.19 μm) were analyzed with respect to surface composition by static TOF-SIMS. Positive secondary ion mass spectra were measured from several areas of 500 × 500 μm^2, using a 25 keV Ga primary ion beam and a total ion dose of 10^9 ions or less. In addition to mass spectra, the lateral distribution of different ions from the analyzed areas was imaged.

The wettability of the surfaces was investigated at room temperature by static contact angle measurements performed with a goniometer. Two microliter droplets of deionized water were applied at the sample surface by hand with a syringe, and measurements of the contact angle were made on both sides of the two-dimensional projection of the droplet.

FTIR-RAS (films on gold) was used to confirm the chemical structure of the films. The measurements were performed with a Perkin-Elmer system 2000 FT-IR, equipped with a liquid nitrogen cooled MCT detector. A total of 250 scans were recorded at a resolution of 4 cm^{-1}.

The average thickness of films thinner than 0.32 μm was measured at 10 different spots on each sample (spot diameter 0.07 mm) with a Rudolf Research AutoEL-II ellipsometer ($\lambda = 633$ nm, assuming $n_{HDPE} \cong 1.54$ and measured $N_{Au} = 0.15 - 3.4j$). Measurements of the average film thickness were also obtained gravimetrically using the microbalance mentioned above, a Q-Sense QCM device[15] (AT-cut quartz sensor, resonant frequency 5 MHz, mass constant $C = 1.8 \times 10^{-13}$ g/(m^2 Hz)). The thickness of films thicker than 0.32 μm was measured with a Tencor Alpha Step 500 surface profilometer.

Optical reflection microscopy (Zeiss, Axiotech 100 DD DIC microscope), in dark field mode or with crossed polarizers, was used to examine general structural features of the films. The surface microtopography and the morphology of the films were measured with a Digital Instruments Nanoscope IIIA atomic force microscope, using a Dimension 3000 large sample type G scanner in tapping mode with a standard silicon tip.

Results and Discussion

Chemical Composition of Films. ESCA characterization of films of different thickness gave spectra typical for HDPE. The relative carbon concentration of the fully covering films was more than 99.3%, while the oxygen concentration was at maximum 0.7%. In accordance with ESCA, the TOF-SIMS analysis showed typical polyethylene spectra, with strong signals for C_nH_{2n-1} ions. A detailed analysis of the spectra also showed weak signals, indicating the presence of oxidation products (e.g., CHO^+, $C_2H_3O^+$, and $C_3H_5O^+$) as well as traces of Na, K, and Si. Ion images revealed that the composition was homogeneous within the resolution used in the analyses (∼1 μm), with the exception of occasional pits where elevated Si levels were detected. The latter most likely represent pinhole defects in the films. FTIR-RAS showed only the three most characteristic hydrocarbon peaks of HDPE at 2923, 2849, and 1473 cm^{-1}. Goniometer measurements on the HDPE films with water resulted in a static contact angle of 95° (±3, $n = 18$), which corresponds to a hydrophobic surface.

Spin Coating of Films and Film Thickness. There are several reasons for the choice of spin coating HDPE at a high temperature, 180 °C. When we started the spin-coating experiments, we found that avoiding early phase separation was crucial to obtain smooth and uniform films and that preheating of substrates and equipment was necessary. Working near the boiling point of the solution ensured a constant initial deposi-

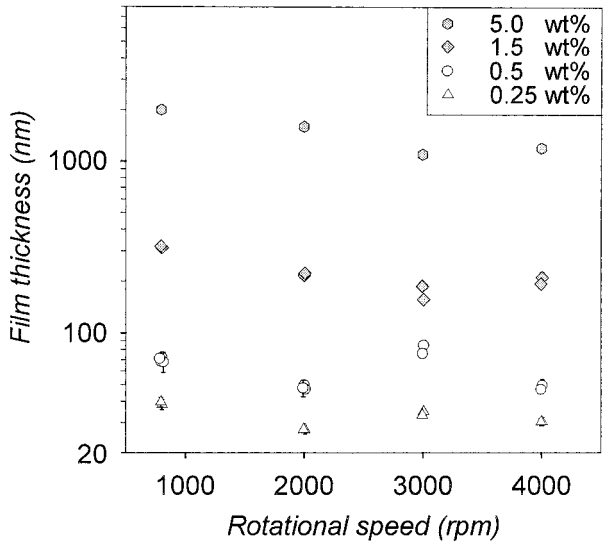

Figure 1. HDPE spin-coated on silicon wafer at the initial deposition temperature of 180 °C. Film thickness vs rotational speed at different polymer concentrations. The standard deviation for each point is shown as vertical error bars for all concentrations, except the 5 wt % solution. Missing error bars indicate that the deviation is less than the size of the point.

tion temperature and prevented early crystallization. However, complementary coating experiments at lower temperatures (down to 100 °C) were performed. Despite the necessity of working at elevated temperatures, the spin-coating technique was found to be a relatively simple way to reproducibly prepare macroscopically smooth thin films of high-density polyethylene of a given thickness.

To produce films of different thickness, the concentration of the polymer solution and the spinning rate were varied. As seen in Figure 1, the former had a much greater influence on the film thickness than the latter. Plots of initial polymer concentration vs film thickness (not shown) also support this. The effect of the rotational speed was significant only below 2000 rpm. At higher rates, the decrease in film thickness leveled off, most likely due to the enhanced evaporation rate which increased the viscosity of the solution, thus counteracting the larger shear force on the polymer solution. For the lower concentrations used, the polymer solution readily wetted the silicon substrate, while the viscosity was so high for the 5 wt % solution that an excess of solution was needed to achieve complete coverage of the substrate.

To investigate the influence of solvent evaporation rate on film thickness, we performed experiments at different temperatures. As shown in Figure 2, the film thickness decreased with decreasing process temperature. The decline in film thickness can be explained by a reduction in the evaporation rate, which maintained lower viscosity of the solution during a longer time period, thus resulting in further thinning of the film. This reasoning is consistent with the results of several studies focused on the relationship between final film thickness and solvent volatility.[16−18]

A visual examination of the films spin-coated at 180 °C indicated that a spin speed of 2000 rpm gave the best results with respect to both smoothness and absence of macroscopic defects in the films. The defects, mainly in the form of circular nonpenetrating pits, were probably caused by rapid evaporation. Their number diminished when spin coating was done at lower temperatures.

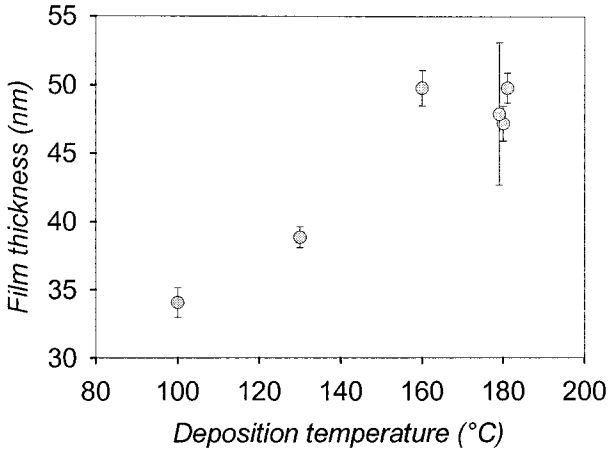

Figure 2. HDPE spin-coated onto silicon wafer at different deposition temperatures. Film thickness vs deposition temperature (polymer concentration 0.5 wt %), rotational speed 2000 rpm.

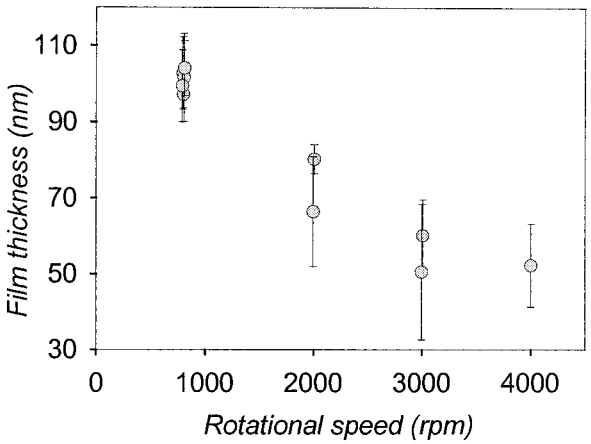

Figure 3. HDPE spin-coated on gold at the initial deposition temperature of 180 °C. Film thickness vs rotational speed, polymer concentration 0.5 wt %. The standard deviation for each point is shown as vertical error bars.

Figure 3 shows the thickness of HDPE films spin-coated onto gold substrates at 180 °C. At lower rotational speeds, the films tended to be slightly thicker than those on silicon wafer. Spin coating the polymer onto the gold electrode of QCM disks provided an alternative method, besides ellipsometry, for estimating the film thickness. It also offers possibilities for future use of the QCM technique in surface modification studies, e.g., cell adhesion on surface-modified polymer coatings.[19] In general, the QCM and ellipsometry measurements gave similar results regarding film thickness. However, in a few cases, greater differences were observed. The causes were identified as contamination of the lower (noncoated) electrode of the QCM disk or as the occurrence of a center defect, as discussed below.

According to AFM analysis, the polymer films spun at 180 °C were continuous at film thicknesses down to at least 50 nm. This result was confirmed by ESCA and TOF-SIMS measurements. Experiments to produce thinner films led to discontinuous coatings. Others have found the lower limit of film thickness for continuous spin-coated films of amorphous polymers such as polystyrene,[20] natural rubber, and poly(methyl methacrylate)[21] to be in the range 2−30 nm. Bartczak et al.[12] reported 15 nm for the semicrystalline polymer HDPE.

The higher value in our study results from the presence of an undulating pattern in the films (discussed below). This is supported by the experiments at 100 °C, in which the films lacked undulations and remained continuous down to the lowest film thickness prepared in this study, i.e., 34 nm. The detailed design of the chuck had effects on the resulting film thickness and uniformity. This is a common problem often encountered in spin coating. The phenomenon has been addressed by Birnie et al.[22] and is caused by a nonuniform lateral temperature distribution between the parts of the substrate resting on the metal and those that are not. In our case, regions of the substrate in contact with the chuck, or in the close vicinity of it, had a slightly different shade owing to variations in film thickness caused by local differences in evaporation rate. The effect was much more pronounced in the films made on gold substrates, where marks picturing the design of the vacuum troughs were reproduced. In the same manner, a defect, perhaps arising from a vortex, could often be observed at the center of rotation of the films on gold if the suction was applied at the center of the chuck. This type of defect was absent in the films coated on silicon wafer. These observations can be explained in terms of heat transfer from the chuck and differences in the thermal conductivity of the substrates.[22] During the course of the spin coating, the evaporation leads to a considerable cooling of the solution and its surroundings. Substrate regions in contact with the metal chuck will be warmer because of the greater heat transfer, thus experiencing a locally higher evaporation rate, which leads to somewhat greater film thickness. The quartz plate on which thin gold film is deposited has a much lower thermal conductivity (about 10^3 times) than silicon and thus cannot distribute the heat as uniformly as silicon does.

General Structure of Films. Optical reflection microscopy and AFM revealed that all the films made at 180 °C, except the thickest ones (>0.32 μm), had pronounced radial striations, i.e., tangentially undulated structures with a typical periodicity of 30−80 μm and an average peak-to-valley height of roughly one-third of the average film thickness. Films prepared on gold substrates had a similar appearance as those on silicon wafers. Higher rotational speeds resulted in a decreased lateral distance between the striations. It was also notable that the undulations still remained after remelting of the films at 180 °C. Typical surface roughness values were $R_a = 4$ nm for a 70 nm thick film on silicon wafer (measured by AFM over an area of 70 × 70 μm) and $R_a = 12$ nm for a 0.22 μm thick film (80 × 80 μm). The films thicker than 0.32 μm had a different surface structure owing to the presence of more three-dimensionally grown spherulites; see below. The radial pattern was not visible in the optical microscope, although some type of radial order could be discerned with the microscope and the cantilever of the profilometer. When performing the spin coating at lower temperatures, we observed that the irregularities diminished; for films spun at 100 °C, the striations were no longer visible in the optical microscope.

The occurrence of surface irregularities has been noted by several authors, especially when using high-volatility solvents.[17,23,24] In addition, Spangler et al.[17] observed that the size of wavelike irregularities in polystyrene films increased when they used a poorer solvent. When the polymer concentration was higher than the critical concentration for entanglements, uniform films were obtained regardless of the characteristics of the three different solvents used. Thus, they proposed that factors affecting the viscosity, such as polymer−solvent interactions, polymer entanglements and solvent volatility, influenced the existence of the waves.

An alternative and more stringent explanation for the appearance of the striations was given by Daniels et al.[25] The thickness variations are thought to be caused by a phenomenon called the Marangoni effect,[26] i.e., surface-tension-gradient driven flow. Evaporation induces temperature gradients or leads to a local enrichment of polymer molecules (or surface impurities) that results in a higher surface tension in the surface layer. This causes an upward flow of solution from areas of potentially lower surface tension. The flow induces a nonuniform concentration across the polymer film, which reduces its free energy by creating hexagonal Bénard cells, in which vertical solution circulation takes place (Bénard instability). According to the hypothesis of Daniels et al., the radial flow during spin coating will suppress the circulation in the radial plane, while tangentially directed flow in the cells still exists. Eventually, the cells are elongated and connected under the action of centrifugal force, forming striations. Several measures, such as the use of low-volatility solvents, surface-leveling agents, solvent mixtures, saturation of the overlaying gas phase, and fast substrate acceleration, have been found to reduce the formation of striations during spin coating of polymer solutions.[24,25,27−29] For the use of colloidal suspensions, high spin speeds and high initial solid concentration have also been shown to have an important effect.[30]

An indication of Bénard instability was observed in the center of our films as traces of irregular cells. In the experiment at low temperature, a decrease in the evaporation rate was probably the main cause of the absence of the striations. Similarly, we found that the striations were reduced when we placed a cup over the substrate during the spin coating, thus maintaining a higher ambient concentration of solvent molecules and decreasing the air convection. Reduced evaporation will decrease the elevated polymer concentration in the surface layer as it lowers the temperature gradient in the liquid film as a result of less evaporative cooling. These diminished gradients will contribute to less vertical flow and therefore suppress the formation of Bénard cells.

Crystal Morphology of HDPE Films Deposited on Silicon Wafer. The morphology of the thinnest films, deposited on silicon wafer at 180 °C, consisted of nonbranched, edge-on oriented lamellae gathered in sheaflike aggregates (Figure 4) very similar to those observed by Bartczak et al.[12] As the film thickness increased, the edge-on orientation of the lamellae became more diffuse (Figure 5), and they formed more conventional, though flattened, polygonal spherulitic structures with a diameter of ∼0.1 mm (Figure 6). AFM analysis of 80 nm thick films indicated that the shift in morphology occurred around a film thickness of 0.1 μm. The lamellae seemed to originate more distinctly from spherulite centers in thicker films. At the ridges of the undulations, corresponding to thicknesses above 0.1 μm, a more twisted appearance was observed, resembling the structure shown in Figure 5, whereas the edge-on lamellae dominated in the valleys (see Figure 4). Still, the spherulite boundaries were diffuse and did not

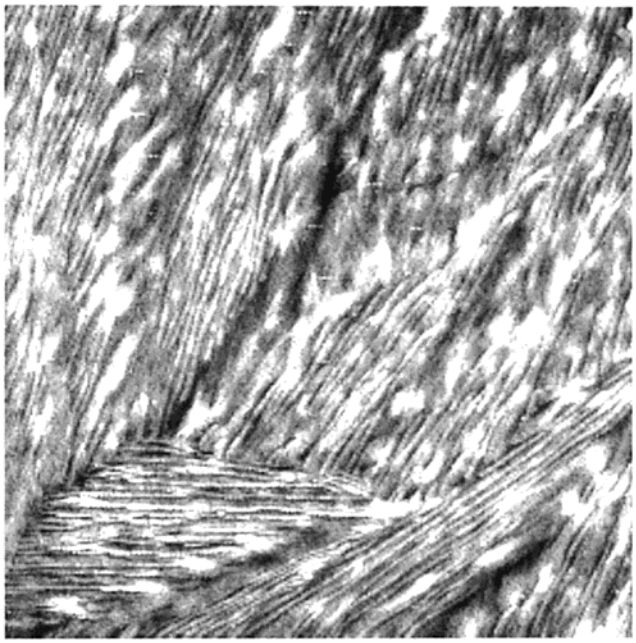

Figure 4. AFM image ($10 \times 10\ \mu m^2$) of a 50 nm thick HDPE film spin-coated on silicon wafer demonstrating the sheaflike structures that prevailed below a thickness of 0.1 μm.

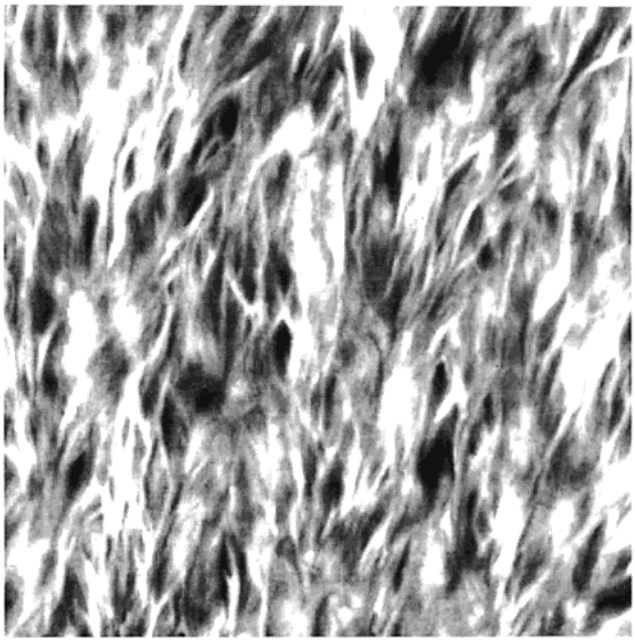

Figure 5. AFM image ($10 \times 10\ \mu m^2$) of a 0.22 μm thick HDPE film on silicon wafer showing more disordered lamellae than those present in thinner films.

become fully clear in the optical microscope until the film thickness was above 0.1 μm. The presence of the sheaflike structures in the thinnest films may possibly be explained by a higher secondary rate of nucleation for the crystals growing edge-on in contact with the substrate.[12] Our observations differ from the results of Bartczak et al.[12] since they noticed the shift in morphology above a film thickness of 0.3 μm. Note however that their observation relates only to remelted films, which were slowly cooled.

When the spin coating was performed at low temperature, 100 °C, the morphology of thin films, thickness 34 nm, changed. Instead of sheaves, a flattened spherulite structure was seen (Figure 7). The absence of edge-on aggregates in this case can be explained by a reduced polymer−substrate interaction; i.e., the polymer crystallized from solution rather than from polymer melt. The spherulites and the lamellae were smaller, which simply reflects lower crystallization temperature.

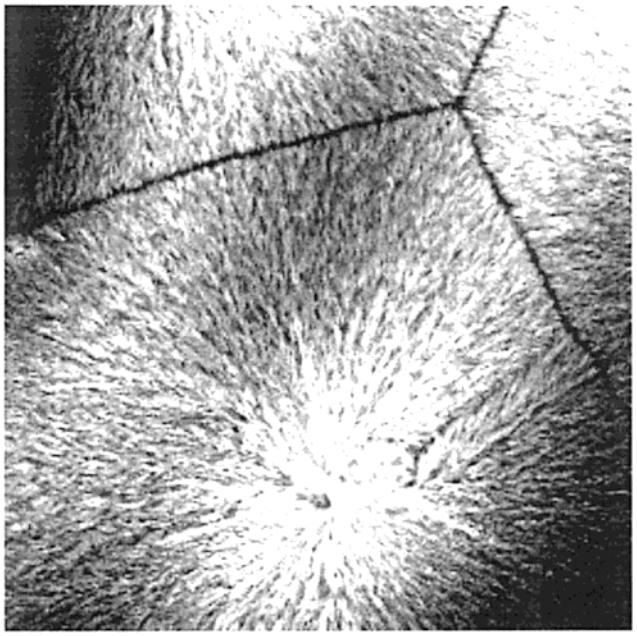

Figure 6. AFM image ($80 \times 80\ \mu m^2$) of a 0.22 μm thick HDPE film on silicon wafer showing both the undulating structure of the film as two ridges and a flattened spherulite with center and boundaries. Bright colors correspond to higher areas.

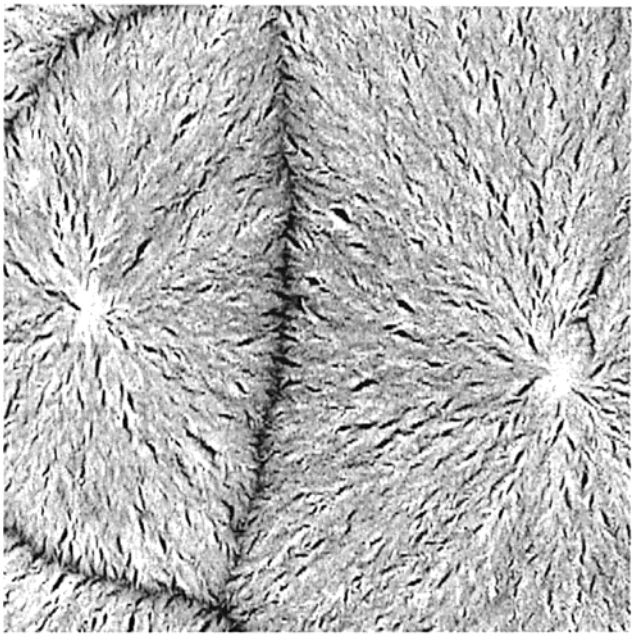

Figure 7. AFM image ($20 \times 20\ \mu m^2$) of a 34 nm thick HDPE film spin-coated on silicon wafer at 100 °C.

The shape and size distribution of the spherulites showed no variations that could be associated with the rotational speed during spinning. For the thickest films, distinctly banded spherulites were observed with AFM and optical microscope (crossed polarizers). The banding, a common phenomenon known to occur at supercooling (particularly when $\Delta T > 15$ °C), is caused by giant screw dislocation of radially growing lamellae.[31,32] The characteristic extinction pattern of the banding became weaker as the film thickness decreased (Figure

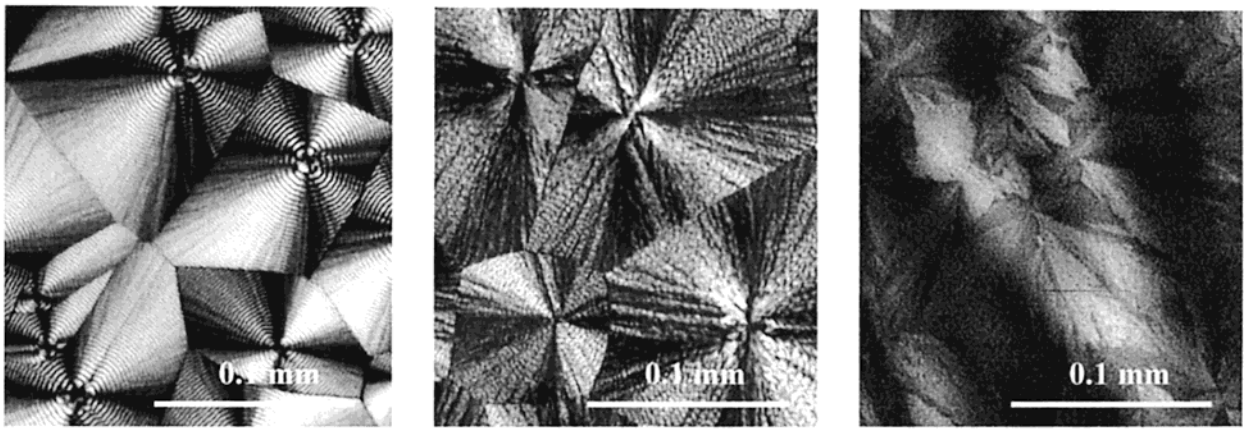

Figure 8. Optical micrographs (crossed polarizers) of three HDPE films on silicon wafer. Film thickness: (a) 2 μm, (b) 0.31 μm, (c) 70 nm. The banding of the spherulites diminishes as the film thickness decreases.

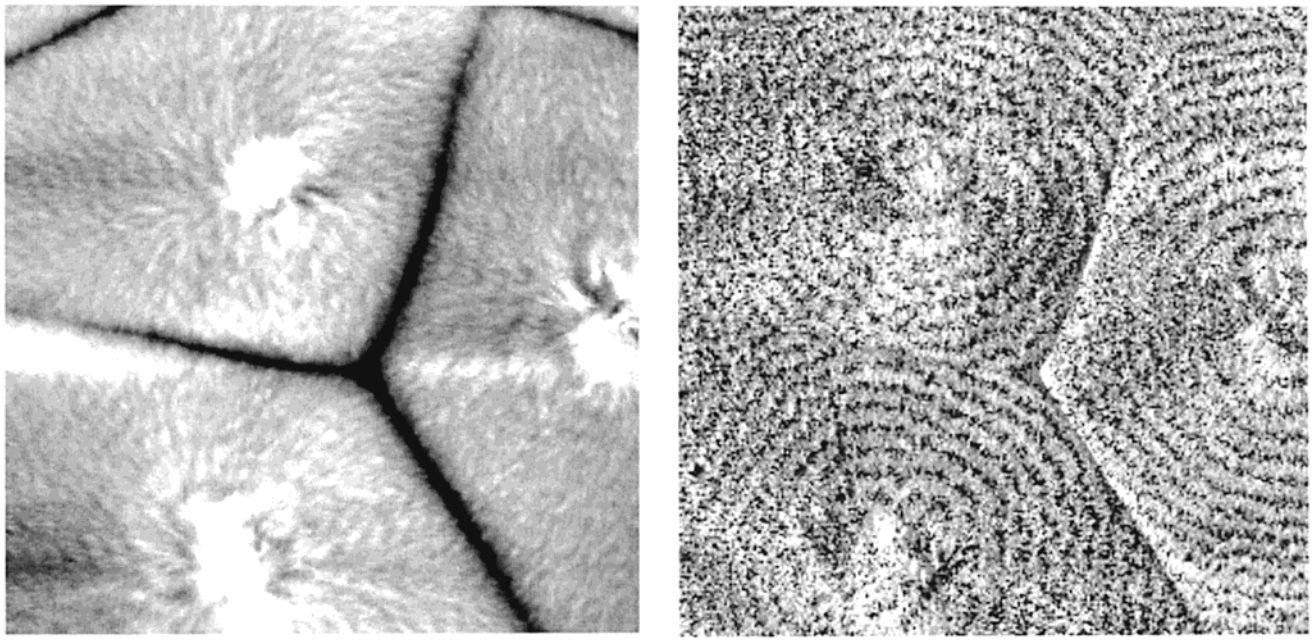

Figure 9. AFM images (70 × 70 μm^2) of a 1.6 μm thick HDPE film on silicon wafer (a) height image and (b) phase image.

8). Figure 9 demonstrates AFM images of banded spherulites in a 1.6 μm thick film. The bands are much more easily distinguished in the phase image because the crystal edge and the noncrystalline folded surface of twisting lamellae give phase contrast owing to differences in properties.

Remelting of films on silicon wafers followed by slow cooling did not result in any significant change in spherulite size or morphology. For the thinnest films, AFM showed that the structure of the lamellae was practically unchanged although dewetting was observed. The change in morphology, from sheaves to spherulites, did not occur at a greater film thickness as one might have expected considering the work of Bartczak et al.[12] However, the band spacing increased from 1 to 2 μm to 6−7 μm, and the banding became less regular in the thickest films, while it disappeared in the thinner ones. The larger band spacing and the partial disappearance of the bands upon remelting indicate that the conditions during remelting were much closer to equilibrium than they were during spinning. There are two possible causes for the observation of fainter banding in the thinner films. First, it is apparent that the substrate suppresses the lamella twisting, as a preferential edge-on orientation exists for lamella grown at the interface. At higher crystallization temperatures, this orientation persists at a larger film thickness, which is revealed when studying remelted films. Second, thicker films permit growth of larger lamellae, e.g., in a second layer, which provide more contrast-yielding material of twisting lamellae.

Crystal Morphology of HDPE Films Deposited on Gold and on SiO_2-Coated Substrates. We have up to now described HDPE deposition and film morphology for two different substrates, mainly the silicon wafer and few observations relating to gold (evaporated onto quartz). These two substrates differ from each other in three main aspects with regard to morphology and crystal structure of the coated HDPE films: (i) the heat conductivity difference leads to different substrate surface and film temperatures during spinning, and thus different crystallization temperatures, (ii) different chemistries (Au vs thermally oxidized Si) may result in different wetting of solute and solvent, or differences in lattice parameters may influence the molecular arrangement, and finally (iii) difference in surface roughness or surface defect density may result in different densities of the nucleation sites or it may affect

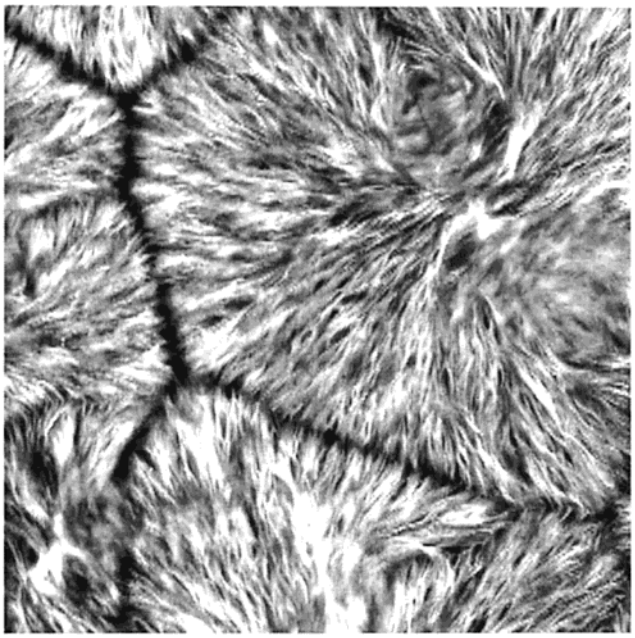

Figure 10. AFM image ($30 \times 30\ \mu m^2$) of a $0.3\ \mu m$ thick HDPE film on gold.

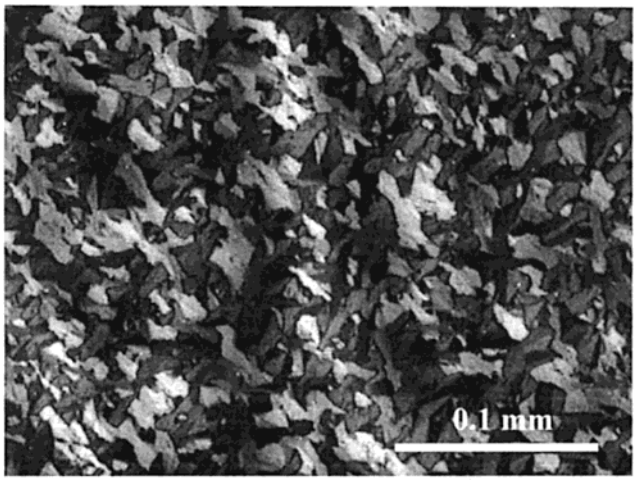

Figure 11. Optical micrograph (crossed polarizers) of $0.1\ \mu m$ thick HDPE film on gold.

the crystal growth. To elucidate the relative importance of these factors, chemically similar surfaces were prepared on each of the two substrates by evaporating thin SiO_2 films prior to spin coating. In addition, few experiments were performed on oxygen plasma treated silicon wafers, a procedure known to result in thin SiO_2 surface layers. AFM analysis of the substrates ($1 \times 1\ \mu m^2$) resulted in the following roughness values: $R_a = 0.33$ nm for untreated wafer, $R_a = 0.14$ nm for oxygen plasma treated wafer, and $R_a = 0.88$ nm for the silicon dioxide coated wafer. Similarly, the gold substrates were measured: $R_a = 1.9$ nm for untreated and $R_a = 1.4$ nm for silicon dioxide coated.

Spherulites observed in the thick HDPE films on gold substrate were approximately 4 times smaller than the ones on silicon wafer and appeared less regular in the optical microscope (Figure 10). In the thinnest films the sheaflike aggregates were smaller and more distinct (Figure 11) than compared to the films deposited on silicon wafer (Figure 8c). The higher number of spherulites on the gold substrate implies a higher density of nucleation sites than on the silicon wafer. This difference can be due to diverse crystallization temperatures caused by different heat conductivities of the two substrates and/or different nucleation abilities of the substrates owing to differences in surface properties. To investigate the relative importance of temperature and substrate effects, remelted films were studied. Upon remelting, the HDPE films on gold showed a 2−3-fold increase in the crystal aggregate size, while it remained virtually unchanged for films on silicon wafer. These observations indicate that the difference in spherulite size on the two substrates is partly due to effects of the substrate surface. As seen in Figures 6 and 10, the spherulite centers and the growth mechanism in films on silicon wafer and gold, respectively, appear different. The spherulites on the former have a more central multidirectional growth, while on the latter substrate, the growth is sheaflike and unidirectional.[33] Both types of structures remain after remelting.

To further study the substrate influence on crystallization, the SiO_2-coated gold substrates (QCM disks) were spin-coated. For the thinnest polymer films, we observed a striking difference in aggregate size when comparing with films on the original gold surface, in that the film on the SiO_2 surface showed features similar to those found on films deposited on silicon wafer. The spherulites in the thicker films resembled those found in thicker films on gold, which had a unidirectional growth pattern. Remelting of the films did not change the unidirectional growth on gold, but on the SiO_2-coated substrate the crystal expansion was altered dramatically and the spherulites turned into starfish-shaped structures with a diameter of 0.1 mm. About four to six fibrils, 3 μm wide, grew out of crystallite centers, consuming most of the material and leaving a thin layer of disordered lamellae or uncovered substrate in between.

For silicon wafers treated by oxygen plasma or coated by silicon dioxide, no difference in polymer morphology in the as-casted films was observed, as compared to nontreated wafers. However, in the remelted films the spherulite growth was once again starfish-shaped and more pronounced on the plasma cleaned wafer than on the SiO_2-coated one.

These experiments indicate that the substrate has a great impact on polymer crystallization in thin films, especially at low supercooling. Evidently, there is an effect of the molecular structure of the surface; i.e., the polycrystalline gold has more nucleation sites than the various amorphous, silicon oxide substrates. Further on, it is most likely that the nucleation on the silicon oxide substrates was induced by foreign particles in the polymer material, e.g., catalyst fragments, and not by the surface as the amount of nucleating sites are more or less constant regardless of oxide type. If the silicon wafer would have had a specific distribution of activating defects, it is unlikely that it would remain after changing the surface by evaporation of silicon dioxide.

More unexpected was the influence of different substrate topographies. Even with a thin layer of silicon dioxide on top, the rougher features on gold seem to guide the crystal growth unidirectionally. At low cooling rates this effect vanishes, and the growth is governed more by the chemical nature of the surface. One can only speculate whether or not there is an influence of the surface roughness and/or possible chemical effect that governs crystallization on the different silicon substrates. The two treated silicon wafers are presum-

ably more alike with respect to chemical composition, i.e., same type of silicon oxide, compared to the untreated wafer, which has a more complex composition. At low supercooling, the growth of the lamellae on the two treated silicon substrates differs in terms of branching, possibly because the rougher silicon dioxide coated surface provides more secondary nucleation sites, which induce splaying of the lamellae.

Comparing rubber and calcite substrates, Bartczak et al.[12] claimed that the nucleation could be considered to be initiated by the substrate but that the effect of the substrate on the crystal growth was essentially the same. Nevertheless, our findings suggest that the crystallization, both nucleation and growth, are indeed affected by the type of substrate used. Particularly at low supercooling, even a minor surface modification on an apparently, weakly interacting substrate, such as amorphous silicon dioxide, has a profound influence on the crystallization.

Conclusions

There is a great interest for thin polymer films nowadays, not only for their, in some cases, unique properties but also for their applications in for example the microelectronic industry. This interest also regards semicrystalline polymers, which are less studied, particularly concerning spin coating. In this paper, we have presented a reproducible method for preparing supported thin (0.03−2 μm) films of HDPE on silicon wafers and on gold substrates using spin coating. A variety of experimental techniques were used to characterize these films with regard to the chemical composition, thickness, and morphology. The experiments showed that the deposition temperature, besides the initial polymer concentration, is an important process parameter, mainly because it affects the solvent evaporation rate. A reduced evaporation rate leads to a lower polymer concentration, which results in a decrease in solution viscosity and thus a thinner film. In addition, lower deposition temperatures gave more uniform films and suppressed the formation of radial striations, which allowed production of continuous films of lower final film thickness. It should be noted that existing models for predicting final film thickness were developed for spin coating at room temperature. These models are, however, not valid in this case since spin coating with hot equipment at ambient temperature involves significant changes in evaporation and cooling rate.

Below a film thickness of 0.1 μm, the morphology was composed of aggregates of edge-on oriented lamellae instead of the flattened spherulitic structure observed in thicker films. This thickness dependence of the morphology ceased when the spin coating was performed at the lowest process temperature, as crystallization probably occurred in the presence of solvent, rather than via a polymer melt, that promoted spherulitic growth.

The results also show that the substrate can have a great influence on nucleation and crystal growth, and such changes in polymer morphology may lead to altered film properties. Consequently, it is very important when working with thin films of semicrystalline polymers, e.g., using spin coating, to have control of both the substrate surface and the process conditions in order to obtain reproducible results.

To summarize, we have shown that spin coating, when used with care, is a suitable deposition technique also for highly crystalline polymers, which are not soluble at ambient temperature. The films can be deposited at various substrates, such as the gold electrode of QCM disks, for studying for example biomolecule adsorption and cell behavior in the case of modified film surfaces. Plasma modifications of these types of polymer films are presently being investigated.

Acknowledgment. Financial support from the Swedish Foundation for Strategic Research is gratefully acknowledged. We thank Marie Björklund at the Department of Polymer Technology (Chalmers University of Technology) for skillful operation of the AFM equipment.

References and Notes

(1) Prest, W. M.; Luca, D. J. *J. Appl. Phys.* **1980**, *51*, 5170.
(2) Despotopoulou, M. M.; Frank, C. W.; Miller, R. D.; Rabolt, J. F. *Macromolecules* **1996**, *29*, 5797.
(3) Forrest, J. A.; Dalnoki-Veress, K.; Dutcher, J. R. *Phys. Rev. E* **1997**, *56*, 5705.
(4) Muratoglu, O. K.; Argon, A. S.; Cohen, R. E.; Weinberg, M. *Polymer* **1995**, *36*, 921.
(5) Bartczak, Z.; Argon, A. S.; Cohen, R. E.; Weinberg, M. *Polymer* **1999**, *40*, 2331.
(6) Strålin, A.; Hjertberg, T. *J. Adhes. Sci. Technol.* **1992**, *6*, 1233.
(7) Cranfill, B. *Rev. Sci. Instrum.* **1978**, *49*, 264.
(8) Lopez, G. P.; Ratner, B. D. *J. Polym. Sci., Polym. Chem.* **1992**, *30*, 2415.
(9) Inagaki, N. *Plasma Surface Modification and Plasma Polymerization*; Technomic Publishing Company, Inc.: Lancaster, 1996.
(10) Bornside, D. E.; Macosko, C. W.; Scriven, L. E. *J. Imag. Technol.* **1987**, *13*, 122.
(11) Lawrence, C. J. *Phys. Fluids* **1988**, *31*, 2786.
(12) Bartczak, Z.; Argon, A. S.; Cohen, R. E.; Kowalewski, T. *Polymer* **1999**, *40*, 2367.
(13) Kressler, J.; Wang, C. *Langmuir* **1997**, *13*, 4407.
(14) Mellbring, O.; Kihlman, S.; Krozer, A.; Lausmaa, L.; Hjertberg, T. *Abstr. Pap. Am. Chem. Soc.* **1999**, *217*, 275-PMSE.
(15) Sauerbrey, G. Z. *Z. Phys.* **1959**, *155*, 206.
(16) Chen, B. T. *Polym. Eng. Sci.* **1983**, *23*, 399.
(17) Spangler, L. L.; Torkelsson, J. M.; Royal, J. S. *Polym. Eng. Sci.* **1990**, *30*, 644.
(18) Skrobis, K. J.; Denton, D. D.; Skrobis, A. V. *Polym. Eng. Sci.* **1990**, *30*, 193.
(19) Fredriksson, C.; Kihlman, S.; Rodahl, M.; Kasemo, B. *Langmuir* **1998**, *14*, 248.
(20) Stange, T. G.; Mathew, R.; Evans, D. F. *Langmuir* **1992**, *8*, 920.
(21) Extrand, C. W. *Langmuir* **1993**, *9*, 475.
(22) Birnie, D. P.; Zelinski, B. J. J.; Marvel, S. P.; Melpolder, S. M.; Roncone, R. L. *Opt. Eng.* **1992**, *31*, 2012.
(23) Lai, J. H. *Polym. Eng. Sci.* **1979**, *19*, 1117.
(24) Müller-Buschbaum, P.; Gutmann, J. S.; Wolkenhauer, M.; Kraus, J.; Stamm, M.; Smilgies, D.; Petry, W. *Macromolecules* **2001**, *34*, 1369.
(25) Daniels, B. K.; Szmanda, C. R.; Templeton, M. K; Trefonas, P. *Adv. Resist Technol. Processing III Proc. SPIE* **1986**, *631*, 192.
(26) Scriven, L. E.; Sternling, C. V. *Nature (London)* **1960**, *187*, 186.
(27) Elliot, D. E.; Hockey, M. A. *Solid State Technol.* **1979**, *22*, 53.
(28) Du, X. M.; Orignac, X.; Almeida, R. M. *J. Am. Ceram. Soc.* **1995**, *78*, 2254.
(29) Frasch, P.; Saremski, K. H. *J. Res. Dev.* **1982**, *26*, 561.
(30) Rehg, T. J.; Higgins, B. G. *AIChE J.* **1992**, *38*, 489.
(31) Geil, P. H. *Polymer Single Crystals*; Wiley-Interscience: New York, 1963.
(32) Bassett, D. C. *Principles of Polymer Morphology*; Cambridge University Press: Cambridge, 1981.
(33) Norton, D. R.; Keller, A. *Polymer* **1985**, *26*, 704.

MA000094X